Irradiation-induced amorphization of graphite: a dislocation accumulation model

Keisuke Niwase
Department of Physics, Hyogo University of Teacher Education, Yashiro, Hyogo 673-1494, Japan

ABSTRACT

We present a kinetic model to explain irradiation-induced phenomena in graphite up to a high dose of amorphization. We attribute the origin of amorphization to the accumulation of dislocation dipoles instead of a disordered region assumed in a previous model (Niwase 1995). Calculated results for the change in a sample dimensions up to amorphization and the Raman intensity ratio in a low-damage range, compare favourably with the experimental results, revealing the existence of a barrier inhibiting the mutual annihilation of an interstitial and a vacancy.

1 . INTRODUCTION

Graphite can be amorphized under high-energy particle irradiation with ions (Elman, Dresselhaus, Dresselhaus, Maby and Mazurek 1981, Niwase, Sugimoto, Tanabe and Fujita 1988), neutrons (Niwase, Nakamura, Shikama and Tanabe 1990) or electrons (Nakai, Kinoshita and Matsunaga 1991, Takeuchi, Muto, Tanabe, Arai and Kuroyanagi 1997). Amorphization appears to occur when samples are irradiated to a dose of about 1 displacement per atom (dpa) at room temperature, judging from the appearance of the halo pattern in the transmission electron microscope (TEM) diffraction pattern observed along the original c-axis and a remarkable broadening of the Raman spectra. However, high-resolution transmission electron microscopy (HREM) investigations have revealed that the irradiated graphite still possesses a nanoscale layered sequence along the original c-axis at around 1 dpa (Tanabe, Muto and Niwase 1992, Koike and Pedraza 1994, Muto and Tanabe 1997). At a higher dose of 6 dpa, on the other hand, this layered sequence disappears (Koike and Pedraza 1994).

Recent progress in experimental and theoretical analyses by Raman spectroscopy (Niwase, Tanabe and Tanaka 1992, Nakamura and Kitajima 1992, Niwase 1995, Kitajima 1997) has allowed us to investigate the irradiation-induced phenomena from the viewpoint of in-plane defects of vacancies and their clusters. Based on the change in the Raman spectra during irradiation, a model of irradiation-induced amorphization has been proposed with the following assumptions (Niwase 1995):

(a) The concentration of single vacancies saturates at $C_{VS}(T)$ at an irradiation temperature T after an irradiation time t_1;

(b) Graphite structural regions with single vacancies gradually transform into disordered regions, the accumulation of which leads to the amorphization. The transformation rate is proportional to $C_{VS}(T)$.

According to (a) and (b), the concentration of disordered regions C_D at an irradiation time t_2 can be approximated by

$$C_D(t_2) \propto C_{VS}(T)\, t_2. \qquad (1)$$

The model has successfully predicted the temperature dependence of the critical dose for amorphization and provides the activation energies of the mobilities of single interstitials and di-interstitials. However, it cannot predict the change of the defect concentration under irradiation nor give information on the structure of the disordered region. In this letter, assigning the disordered region to a dislocation dipole (collapsed line) (Kelly, Martin, Price and Bland 1966, Horner and Williamson 1966), we present a kinetic model which can predict the change of defect concentration and give an insight into the disordering process of irradiated graphite.

2. DISLOCATION ACCUMULATION MODEL

The present model generalizes a well-known rate equation describing radiation damage, taking into account the point defects and defect clusters shown in fig.1. The primary dynamic variables are the fractional concentrations of interstitials and vacancies, denoted by C_I and C_V, respectively. Spatial

information is omitted in this mean-field theory. We consider the following five processes that determine C_I and C_V:

Frenkel pair production. An incident atom knocks on host atoms at a rate P, resulting in the formation of a Frenkel pair (interstitial and vacancy). The fraction of atomic sites at which Frenkel pair production can take place is $1 - C_V - C_{VC}$ where C_{VC} is the fractional concentration of lattice sites lost by the formation of dislocation dipoles. The knocked-on atoms remain as interstitials only when they escape mutual annihilation with vacancies.

Mutual annihilation. An interstitial in a recombination volume Z_0 around a vacancy annihilates with a recombination probability q, which depends on the parameters of the barrier for mutual annihilation.

Diffusion. Two-dimensional movement of a single interstitial parallel to the basal plane takes place with a mobility M_I characterized by a migration activation energy E^I_m as $\nu \exp(-E^I_m/kT)$ where ν and k are a frequency factor and the Boltzman constant, respectively. Other movements of interstitials and vacancies parallel to the basal plane and along the c-axis are neglected owing to the high activation energies (Thrower and Mayer 1978).

Interstitial clustering. We neglect the formation of interstitial clusters and loops except for di-interstitials.

Vacancy clustering. Di-vacancies are formed when knock-ons occur at sites close to single vacancies. They grow as dislocation dipoles (collapsed lines) by successive knock-ons close to the ends of collapsed lines and collapse to the basal planes. Neither the di-vacancies nor the dislocation dipoles can annihilate with interstitials (Kelly, Martin, Price and Bland 1966, Horner and Williamson 1966).

Given the foregoing, the rate equations for the concentrations of interstitials (C_I), vacancies (C_V), di-interstitials (C_{2I}), dislocation dipoles (C_C), and vacant lattice sites in the dislocation dipole (C_{VC}) are

$$dC_I/dt = P(1 - C_V - C_{VC})(1 - qZ_0C_V) - q\,Z_0M_IC_IC_V - 2Z_1M_IC_I^2 \quad (2)$$

$$dC_V/dt = P(1 - C_V - C_{VC})(1 - qZ_0C_V) - q\,Z_0M_IC_IC_V - 2Z_2PC_V - Z_2Z_3P^2 \int C_V dt \quad (3)$$

$$dC_{2I}/dt = Z_1M_IC_I^2 \quad (4)$$

$$dC_C/dt = Z_2PC_V \quad (5)$$

$$dC_{VC}/dt = 2Z_2PC_V + Z_2Z_3P^2 \int C_V dt. \quad (6)$$

3. RESULTS AND DISCUSSION

Figure 2 compares the dimensional change in highly oriented pyrolytic graphite (HOPG) along the c-axis during 300 keV electron irradiation at room temperature (Koike and Pedraza 1994) with the results calculated by the present theory using several values of q. The parameters used in the calculations are $Z_0 = 1$, $Z_1 = 1$, $Z_2 = 1$, $Z_3 = 1$ and $\nu = 10^{12}$ s^{-1}. The effect of the values of Z_1, Z_2 and Z_3 will be described elsewhere but the main features discussed in the following are mostly unchanged for values lying between 1 and 3. The value taken for E^I_m is 0.33 eV (Niwase 1997). The dimensional change along the c-axis, $\Delta L_c/L_{co}$, for the calculations is assumed to increase proportionally with the accumulation of di-interstitials, i.e., $(1/L_{co})d\,\Delta L_c/dt = 2J(dC_{2I}/dt)$, where ΔL_c and L_{co} are the change and the original length of the sample along the c-axis, respectively. J is a parameter representing the expansion rate per atom by the formation of di-interstitials. The effect of single interstitials is omitted as their concentration is negligibly smaller than that of the di-interstitials when the dimensional change appears. The agreement is quite acceptable with the values of $q = 5.0 \times 10^{-4}$ and $J = 4.2$ for the two stages of the initial fast elongation up to a dose of 0.2 dpa and the subsequent linear elongation up to 4.0 dpa. The final saturation of the c-axis expansion also appears in the calculation, but the saturation level is higher than that of the experimental result. With smaller values of q, the saturation level can be lowered, but then the deviation from the linear elongation appears too early. The saturation occurs because of a reduction in the number of lattice sites at which Frenkel pair production takes place, i.e., the term $(1 - C_V - C_{VC})(1 - qZ_0C_V)$ in Eq.(2) becomes significant.

The value of the expansion rate $J = 4.2$ is acceptable in its order of magnitude compared to the case of no barrier ($q = 1$) where J has to take an unacceptable high value of 10^3 to accord with the experimental result of the dimensional change. Nevertheless, $J = 4.2$ is larger the value $J = 1$ expected for the case when di-interstitials do not induce excess expansion. This may occur in cases where the di-interstitials make bonds to effectively expand the lattice or dislocation dipoles induce buckling of the basal planes. Also, vacancies may strain the lattice in the basal plane. Further investigation is needed on this subject.

In fig. 3, the real-time change in the Raman intensity ratio of the original graphite peak and the defect peak, I_D/I_G, under ion irradiation at room temperature for two different production rates of 7.0×10^{-7} and $6.7 \times$

10^{-6} dpa/s (Nakamura and Kitajima 1992) are compared with the present theory. Nakamura and Kitajima (1992) found a square-root dependence of I_D/I_G versus irradiation dose and explained this result by a reduction of the phonon correlation length due to vacancy formation. To exhibit a square-root dependence, the vacancy concentration C_V should increase proportionally with the irradiation dose (Nakamura and Kitajima 1992), i.e., the rate of mutual annihilation of a vacancy and an interstitial should be negligibly small. Utilizing the proper value of $q = 5.0 \times 10^{-4}$ obtained from fig. 2, the calculated results can be fitted to the experimental results showing square-root dependencies. The downward deviation from the square-root dose dependence for the upper result can be simulated in the calculation. With a value of $q = 5.0 \times 10^{-4}$, we can write a useful relation to estimate C_V quantitatively from the Raman intensity ratio in the case where most of the in-plane defects are single vacancies:

$$C_V = 0.0016\ (I_D/I_G)^2. \quad (7)$$

Now, we analytically explain the change of vacancy concentration C_V and give an insight into the disordering process of graphite during irradiation. The first terms in Eqs. (2) and (3) are approximated as P for simplification hereafter. In fig. 4, the calculated result of vacancy concentration C_V for the simulation of the dimensional change is shown as a function of dpa. It steeply increases to a critical dose of about 0.4 dpa and then gradually decreases after passing through a maximum. The peak values of the vacancy and interstitial concentrations (C_{Vp} and C_{Ip}) can be approximately estimated for conditions: $dC_I/dt = 0$, $dC_V/dt = 0$ and $dC_{2I}/dt = k$ where the fourth term in Eq. (3) is negligible and the value of k is constant after the peak when the dimensional change shows a linear elongation. The solutions are $C_{Ip} = (k/M_I)^{1/2}$ and $C_{Vp} = k/Z_2P$.

We find that the dose range of the Raman measurements (Nakamura and Kitajima 1992) shown in fig. 3 corresponds to the time before C_V reaches the peak and increases proportionally to the irradiation time, i.e.,

$$C_V = Pt. \quad (8)$$

as seen in fig. 4. This is the reason why the Raman intensity ratio exhibited the square-root dependence. To obtain the linear relationship, a very small value of the recombination probability, q, between a vacancy and an interstitial, i.e., a strong barrier for the mutual annihilation, is needed as described before.

The linear elongation of the c-axis expansion (Koike and Pedraza 1994), on the other hand, corresponds to the dose range after the peak of C_V. The mutual annihilation of interstitials and vacancies is dominant near the peak and then Eq. (2) can be approximated as $P - qZ_0M_IC_IC_V \fallingdotseq 0$. Substituting C_{Ip}, and C_{Vp} into this equation, we obtain

$$k = (Z_2P^2/qZ_0)^{2/3}\ M_I^{-1/3}. \quad (9)$$

In the dose range where the dimensional change shows a linear elongation, the amount of interstitials accumulating in di-interstitials almost balances that of vacancies disappearing at the dislocation dipoles, i.e., $dC_{VC}/dt \fallingdotseq 2k$. Therefore, we obtain $2Z_2PC_V + Z_2Z_3P^2 \int C_V dt \fallingdotseq 2k$. Solving this equation with $C_V = 0$ ($t = \infty$), we find

$$C_V = (k/Z_2P)\exp(-Z_3Pt/2). \quad (10)$$

We can see that this equation roughly explains the change in C_V after the peak as shown in fig.4. Also, the following relation is deduced, as both the formation rate of the dislocation dipoles, dC_{VC}/dt, and the peak value of vacancy concentration, C_{Vp}, increase proportionally with k,

$$C_{VC} \propto C_{Vp}(T)\ t. \quad (11)$$

Note that the formula is similar to Eq. (1) and this is the reason why the previous model (Niwase 1995) succeeded in explaining the change of Raman spectra using the assumption given in Eq. (1). In addition, the saturation of vacancy concentration C_V at a dose of t_1 assumed in the previous model corresponds to the peak formation of C_V in the present model.

The above analysis depicts a picture of the disordering process of graphite under irradiation, taking into account the accumulation of dislocation dipoles. In the dose range before approaching the peak of C_V at 0.4 dpa, the long-range order of the graphite sheet along the c-axis and the sequence of the 6-menber rings in the basal planes remain as the dislocation dipole formation is negligibly small. With increasing dose, the formation of dislocation dipoles by knock-on process becomes significant due to an increase of vacancy concentration. The accumulation of dislocation dipoles destroys the topological long-range order in the basal plane by introducing mackle, rotation and buckling of the graphite sheets, leading to the fragmentation of the basal planes (Muto, Horiuchi and Tanabe 1999). In the early stage of this process, the irradiation-induced disordered structure would still reflect the original layered structure of HOPG. In fact, a TEM diffraction

pattern of graphite observed along the *c*-axis shows a halo when irradiated to a dose of about 1 dpa, but the sequence of the basal planes remains in the HREM images, which are broken up into small segments (Tanabe, Muto and Niwase 1992, Koike and Pedraza 1994). In the highly accumulated state of the dislocation dipoles, nanocrystallization should become considerable and then the long-range order of the layered structure would disappear as shown by the HREM images of HOPG irradiated to a dose of 6 dpa (Koike and Pedraza 1994). Contrary to the significant role of the dislocation dipoles on the disordering process of the planer structure of HOPG, the formation of dislocation dipoles may play an important role in the generation of the concentric graphitic structure of 'bucky onions' under electron irradiation (Ugarte 1992) in addition to the anisotropical flow of point defects in the concentric shells (Sigle and Redich 1997), because the formation of the dislocation dipoles induces curvature of the graphitic layers.

4. CONCLUSIONS

The irradiation-induced amorphization of graphite is theoretically explained. The amorphization is attributed to the destruction of the topological long-range order due to the introduction of dislocation dipoles, leading to nanocrystalline structure connected by dislocation dipoles. In the course of the simulation of the experimental results of the dimensional change along the *c*-axis and the Raman spectra under irradiation, the existence of a barrier on the annihilation of interstitials at vacancies is revealed. A relation is given for estimating the concentration of vacancies quantitatively from the Raman intensity ratio. The theory is applicable to an irradiation temperature below 573 K and should be modified to take into account the mobility of di-interstitials above 573 K (Niwase 1995). Moreover, the effect of cascade damage should be taken into account in the case where the energy of primary knock on atoms is enough high to affect the amorphization process (Abe, Naramoto, Iwase and Kinoshita 1997). The detailed structure of dislocation dipoles is still an open question.

REFERENCES

Abe, H., Naramoto, N., Iwase, A. and Kinoshita, C., 1997, Nucl. Instrum. Methods B, 127/128, 681.
Elman, B.S., Dresselhaus, M.S., Dresselhaus, G., Maby, E.W. and Mazurek, H., 1981, Phys.Rev.24, 1027.
Horner, P. and Williamson, G.K., 1966, Carbon, 4, 353.
Kelly, B.T., Martin, W.H., Price, A.M. and Bland, J.T., 1966,Philos. Mag. 14, 343.
Koike, J. and Pedraza, D.F., 1994, J.Mater.Res., 9, 1899.
Kitajima, M., 1997, Criti. Rev. Sol. & Mater. Sci., 22, 275.
Muto, S. and Tanabe, T., 1997, Philos. Mag. A, 76, 679.
Muto, S., Horiuchi, S. and Tanabe, T., 1999, J.Electron Microscopy, 48, 767.
Nakai, K., Kinoshita, C. and Matsunaga, A., 1991, Ultramicroscopy, 39, 361.
Nakamura, K. and Kitajima, M., 1992, Phys.Rev.B, 45, 78.
Niwase, K., Sugimoto, M., Tanabe, T. and Fujita, F.E., 1988, J.Nucl.Mater., 155-157, 303.
Niwase, K., Nakamura, K., Shikama, T. and Tanabe, T., 1990, J.Nucl.Mater., 106-108, 170.
Niwase, K., Tanabe, T. and Tanaka, I., 1992, J.Nucl.Mater., 191-194, 335.
Niwase, K., 1995, Phys.Rev.B, 52, 15785.
Niwase, K., 1997, Phys.Rev.B, 56, 5685 .
Tanabe, T., Muto, S. and Niwase, K., 1992, Appl.Phys.Lett., 61, 1638.
Thrower, P.A. and Mayer, R.M., 1978, Phys.stat.sol. a, 47, 11.
Sigle, W. and Redich, Ph., 1997, Phil.Mag.Lett., 76, 125.
Ugarte, D, 1992, Nature, 359, 707.

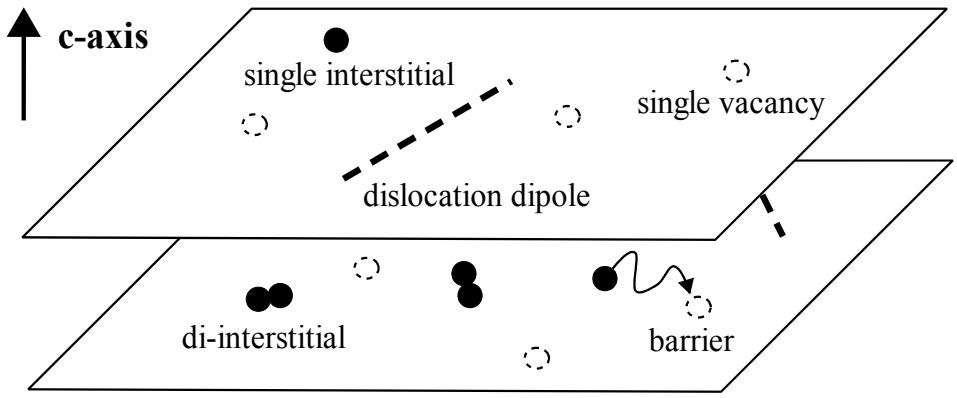

Figure 1 Point defects, defect clusters and their reactions assumed in the present theory. A recombination barrier exists between an interstitial and a vacancy. Di-vacancies are formed when knock-ons occur close to vacancies. They collapse to the basal planes and grow as dislocation dipoles by successive knock-ons close to the ends and are not available to annihilate with interstitial atoms.

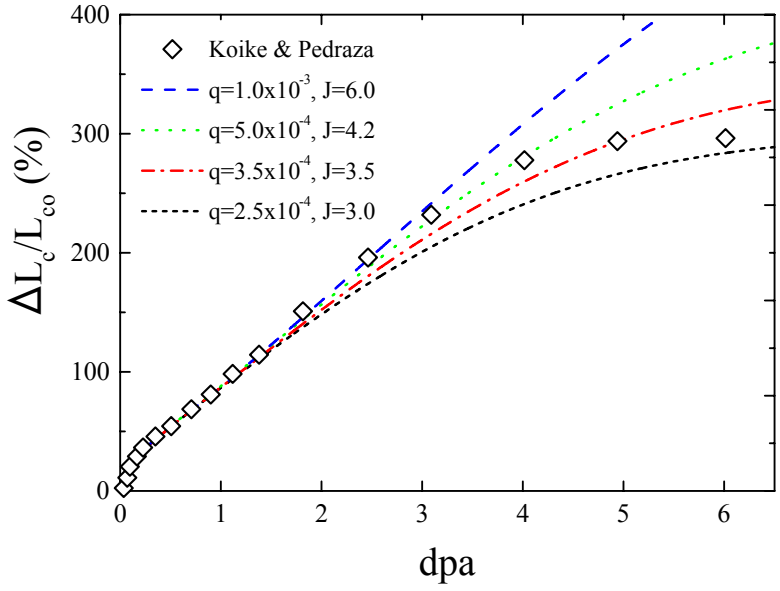

Figure 2 The dimensional change in graphite along the *c*-axis under 300 keV electron irradiation at room temperature (Koike and Pedraza 1994) and the simulation by the present theory with several values of *q*. The dimensional change is assumed to proportionally increase with the amount of di-interstitials accumulated between the basal planes. The value of *J* corresponds to the *c*-axis expansion rate per atom of di-interstitials. The inset shows an enlarged view below 1 dpa.

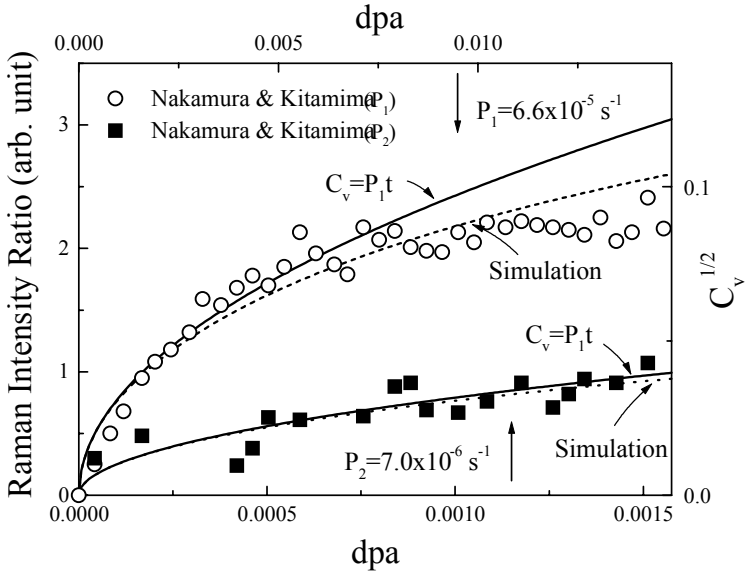

Figure 3 The real time changes of Raman intensity ratio for 3 keV Ar^+ irradiation at room temperature at fluxes of 7.0 x 10^{-7} and 6.7 x 10^{-6} dpa/s (Nakamura and Kitajima 1992). Dotted curves represent the simulation with the present theory and solid curves are the case where all Frenkel pairs remain.

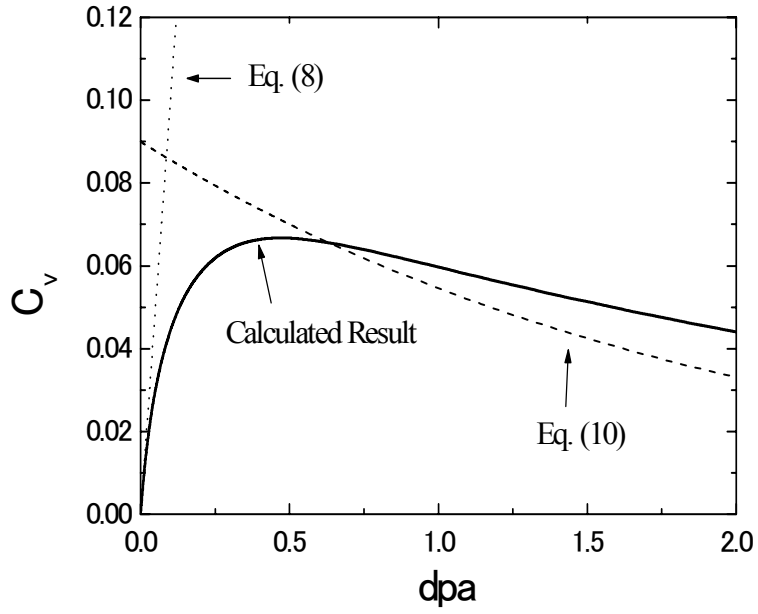

Figure 4 C_V as a function of dpa. Solid curve shows the simulation using the present theory. A dotted line and a broken curve represent analytical solutions give by Eqs. (8) and (10), respectively.